ISSN 1068-7998, Russian Aeronautics (Iz.VUZ), 2013, Vol. 56, No. 2, pp. 111–116. © Allerton Press, Inc., 2013.
Original Russian Text © V.G. Gainutdinov, N.V. Levshonkov, 2013, published in Izvestiya VUZ. Aviatsionnaya Tekhnika, 2013, No. 2, pp. 3–7.

FLIGHT VEHICLE DESIGN

Design of Highly Efficient Propeller Blades

V. G. Gainutdinov and N. V. Levshonkov

Tupolev Kazan National Research Technical University, Kazan, Russia

Received July 2, 2012

Abstract—A technique of evaluating the design parameters for a highly efficient propeller (with optimal geometrical twist) is given. The results of comparative calculations for design parameters of a high-altitude aircraft propeller are presented taking into account air density and compressibility.

DOI: 10.3103/S1068799813020013

Keywords: propeller, optimal geometrical blade twist.

Currently, there is a large interest in the development of high-altitude long endurance Unmanned Aerial Vehicles (UAVs). UAVs are foreseen to operate at altitudes up to 24 000 m, where the density drops to about 3.6 % of the sea level value (the relative air density is about 25 % at cruising altitudes of 12 000 m for passenger airplanes). Improvement of aerodynamic characteristics for such UAVs is of prime consideration. Another important issue is the selection of a power plant. In many cases, priority is given to piston engines with their compressor, turbocharger, heat exchanger, two-stage gear box, efficient propeller, which have a low but constant performance up to altitudes of 24 000 – 26000 m. The propeller operates in the range of air density ratios 1 : 28. With a great variety of flight conditions the effective use of complete motor capacity is a difficult task. Therefore, it is not feasible to choose a propeller that would provide the optimal performance at all flight conditions. In designing the high-altitude UAVs, the designers are forced to make a change from the procedure of propeller selection to its design for specific aircraft and flight conditions. Recently, a large number of works on similar investigations have appeared abroad [1, 2].

The equations of the classical impulse theory for propellers [3] and the blade element theory [4] are used for design evaluation of a propeller. Figure 1 presents a pattern of a flow around the blade cylindrical section in inverse motion. Also shown in Fig. 1 are the specific angles and velocity components.

Let us introduce the following designation: y is the dimensional value of the cylindrical cross-section radius; $r = y/R$ is the relative radius (0–1 or 0–100 %); V is the propeller forward speed; Ω is the angular speed of propeller rotation; v_a and v_t are the axial and tangential components of the induced velocity v; W is the inflow velocity (W_a and W_t are its components); c is the blade section chord; α is the angle of attack; α_i is the angle of induced flow wash; θ is the angle of cross-section setting; δ is the undisturbed flow incidence; ϕ is the disturbed flow incidence. The induced velocity v is perpendicular to the resultant velocity W.

Let us denote by the symbol ζ the ratio of the induced velocity v to the forward speed V. Then we can obtain the following relation (see Fig. 1.)

$$\cos\phi + \zeta = x\sin\phi, \tag{1}$$

where

$$x = \frac{\Omega y}{V} = \frac{\Omega R}{V}\frac{y}{R} = \frac{1}{\lambda_v} r.$$

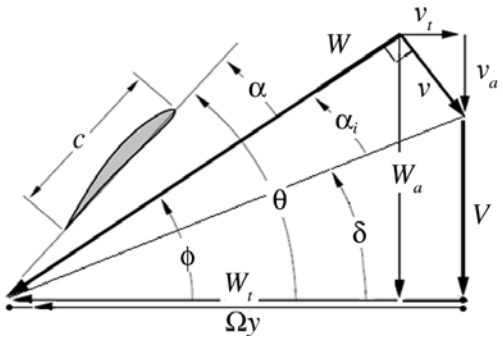

Fig. 1.

Using relation (1), we will calculate the angle ϕ with the rest values of terms entering the formula being specified. If we set the design value of the angle of attack for each blade section $\alpha(r)$, we can evaluate the blade angle $\theta(r)$ (geometric twist) $\theta(r)=\phi(r)+\alpha(r)$.

By comparing the expressions for the lift dY at the blade element cdy

$$dY = C_Y \frac{1}{2}\rho W^2 c dy \tag{2}$$

and for the annular stream filament cross-section

$$dY = 4\pi y \rho v F\left(V + v\cos\phi\right)dy, \tag{3}$$

we obtain the following relation

$$N_b c C_Y W^2 = 8\pi y v F\left(V + v\cos\phi\right), \tag{4}$$

that in the dimensionless form is the following

$$N_b \bar{c} C_Y \overline{W}^2 = 8\pi r F\left(\zeta + \zeta^2\cos\phi\right), \tag{5}$$

where N_b is the number of propeller blades; $\bar{c} = c/R$ is the relative blade chord; $\overline{W}^2 = 3\varsigma^2 + x^2 + 1$; F is the Prandtl loss function [4] that is calculated according to the formula

$$F = \frac{2}{\pi}\arccos\left(e^{-f}\right), \qquad f = \frac{N_b(1-r)}{2\sin\phi_T}, \tag{6}$$

where ϕ_T is the value of the angle ϕ at the blade tip. Further, formula (5) will serve for evaluating the relative chord $\bar{c}$ of the blade cross-sections.

Further, it is necessary to refer the values being specified and obtained to the required thrust T evaluated to fulfill the flight at the specified velocity V and altitude (density) or to the available power on the shaft P. In this regard, use is made of the following equations

$$dT = dY\cos\phi - dX\sin\phi = dY\cos\phi\left(1 - \varepsilon\tan\phi\right); \tag{7}$$

$$\frac{dQ}{y} = \left(dY\sin\phi + dX\cos\phi\right)y = dY\sin\phi\left(1 + \frac{\varepsilon}{\tan\phi}\right), \tag{8}$$

where

$$\varepsilon = \frac{dX}{dY} = \frac{C_X}{C_Y};$$

dQ is the axial moment created by the aerodynamic forces of blade elements and Fig. 2 illustrating them. The triangle of velocities W, W_a, W_t and the aerodynamic forces dX and dY are shown in Fig. 2a and Fig. 2b presents the transition from the aerodynamic forces dX and dY to the thrust dT and axial moment dQ.

After substituting into Eq. (7) or (8) relations (2) and (5) and integrating with respect to the blade radius

$$T - \int_0^R dT = 0 \quad \text{or} \quad P - \int_0^R \Omega dQ = 0, \tag{9}$$

we obtain the quadratic equation of the following form

$$A\varsigma^2 + B\varsigma + C = 0, \tag{10}$$

the solution of which provides some value ζ.

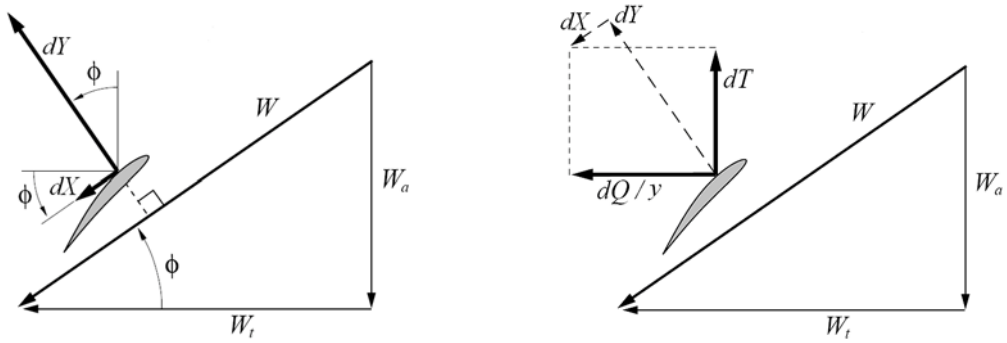

Fig. 2

The value ζ obtained will not coincide with the specified one at the beginning of calculations; therefore, a series of iteration calculations of ζ will be performed until the values ζ being specified and obtained from Eq. (10) turn out to be equal.

Note that the value ζ should be constant over the blade radius according to the condition of propeller optimality [5].

Equations (9) can be presented in the dimensionless form. For this purpose, use is made of the expressions for the coefficient of thrust C_T or power C_P:

$$C_T - \int_0^r dC_T = 0 \quad \text{or} \quad C_P - \int_0^r dC_P = 0; \tag{11}$$

$$dC_T = \frac{dT}{\rho\left(\pi R^2\right)\left(\Omega R\right)^2} = \frac{1}{2} N_b \bar{c} C_Y \overline{W}^2 \lambda_V^2 \cos\phi\left(1 - \varepsilon\tan\phi\right) dr; \tag{12}$$

$$dC_P = \frac{dP}{\rho\left(\pi R^2\right)\Omega^3 R^3} = \frac{1}{2} N_b \bar{c}\, C_Y \overline{W}^2 \lambda_V^2 \sin\phi\left(1 + \frac{\varepsilon}{\tan\phi}\right) r dr. \tag{13}$$

After substituting (5) into Eqs. (12) and (13), we finally obtain

$$dC_T = 4\pi r F \lambda_V^2 \left(\zeta + \zeta^2 \cos\phi\right)\cos\phi\left(1 - \varepsilon\tan\phi\right) dr; \tag{14}$$

$$dC_P = 4\pi r^2 F \lambda_V^2 \left(\zeta + \zeta^2 \cos\phi\right)\sin\phi\left(1 + \frac{\varepsilon}{\tan\phi}\right) r dr. \tag{15}$$

The algorithm described permits the parameters of the optimal propeller to be determined, namely, the chord $\bar{c}$ and geometrical twist $\theta(r)$.

Let us perform the comparative evaluation of the propeller optimal blades according to the preceding scheme for the light aircraft with the ROTAX 914 UL engine: the design speed 216 km/h; the available power on the shaft $P = 74.5$ kW; the shaft revolutions $n_m = 2550$ rev/min; the air density $\rho = 1.225\ \text{kg/m}^3$, the number of blades $N_a = 3$; the propeller diameter $2R = 1.7$ m; NACA 0009 airfoil for all blade cross-sections (between $r = r_0$ and $r = 1$) the design angle of attack $\alpha_d = 5°$; the inner blade radius $r_0 = 0.2$.

Figure 3 presents the graphs of changing the angle ϕ (r) over the blade span for three design values of the radius R, and Fig. 4 shows the change in propeller efficiency η. It is seen that the efficiency of the optimal propeller decreases insignificantly at the lower flight velocities relative to the value for which the propeller is designed.

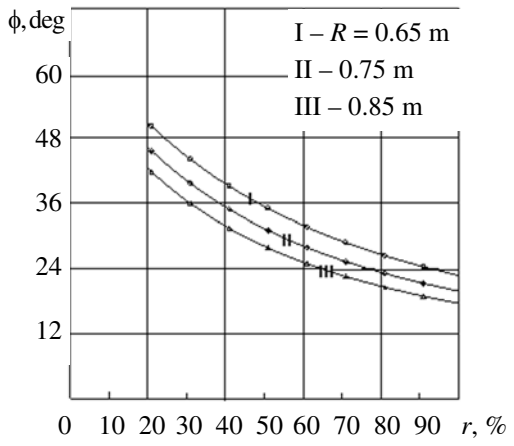

Fig. 3

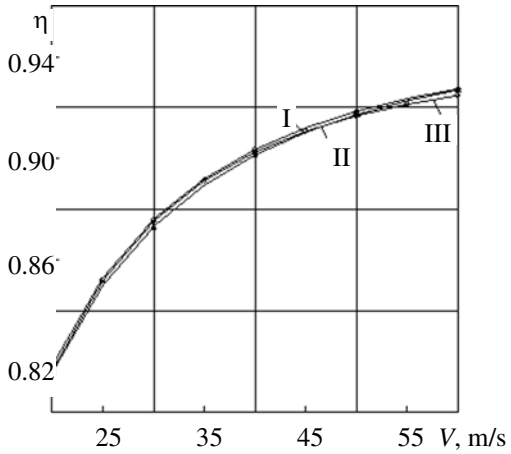

Fig. 4

The air compressibility effect may have a significant influence on the propeller characteristics. The local Mach number along the propeller blade can vary significantly. If the aerodynamic characteristics of airfoils include the dependences on the Mach number, it is necessary to interpolate them over the blade length (as the characteristics on Reynolds number). If the initial data is available only for the low Mach numbers, it is possible to use them for refining the coefficients C_Y and C_X with regard for compressibility.

The design assessment is based on determining the local critical Mach number M_{cr} and the Mach number of abrupt drag increase M_{dr}. The critical number M_{cr} is connected with the minimal airfoil pressure coefficient $c_{p.\,min}$ for incompressible flow by the following relation [4, 5]:

$$c_{p.\,min} = \frac{2\sqrt{1-M_{cr}^2}}{\dfrac{1.4M_{cr}^2}{\left(\dfrac{1+0.2M_{cr}^2}{1.2}\right)^{3.5}-1}+\sqrt{1-M_{cr}^2}-1}. \tag{16}$$

The empirical dependences of the coefficient $c_{p.\,min0}$ on airfoil relative thickness t at an angle of zero lift may be composed. For example, for NACA 0006 – 0018 airfoils we have the following dependence [5]:

$$c_{p.\,min\,0} = -4.764t^2 - 2.266t - 0.070.$$

With the lift force the equation to determine M_{cr} is presented in the following form

$$-4.764t^2 - 2.266t - 0.070 - 0.75\frac{C_Y^2}{t} = \frac{2\sqrt{1-M_{cr}^2}}{\dfrac{1.4M_{cr}^2}{\left(\dfrac{1+0.2M_{cr}^2}{1.2}\right)^{3.5}-1}+\sqrt{1-M_{cr}^2}-1}. \tag{17}$$

In many cases, M_{cr} specifies a threshold after which the compressibility influence cannot be neglected. However, when the relation M/M_{cr} is within the limits 1.04–1.20, the drag grows rather significantly (the value M, for which $dC_d/dM = 0{,}1$ is the Mach number M_{dr} of the drag abrupt rise) specifies the limit after which the aerodynamic characteristics considerably deteriorate). The empirical dependence exists between M_{cr} and M_{dr} [6]

$$M_{dr} = M_{cr}\left(1.04 + 0.4C_Y - 0.25C_Y^2\right) \tag{18}$$

When $M < M_{dr}$, with the Mach number increase the lift coefficient grows due to the air compressibility

$$\frac{C_{Ycomp}}{C_Y} = \frac{1}{\sqrt{1-M^2}} = \beta_{PG}. \tag{19}$$

For $M > M_{dr}$ the lift coefficient decreases with the Mach number increase and has the minimal value at $M \cong 0.9$. The correcting factor is defined by the following expression

$$C_{Ycomp} = C_Y \beta_{KA} \frac{1-M^2}{1-M_{dr}^2}, \tag{20}$$

where $\beta_{KA} = \beta_{PG} + \frac{t}{1+t}\left[\beta_{PG}\left(\beta_{PG}-1\right) + \frac{1}{4}\left(\kappa+1\right)\left(\beta_{PG}{}^2-1\right)^2\right]$; κ is the adiabatic exponent $\left(\kappa \approx 1{,}4\right)$.

The drag C_X does not depend on the Mach number at $M < M_{dr}$, but for $M > M_{dr}$ the additional drag caused by formation of shock waves is given by the expression [6]:

$$C_{Xcomp} = C_X + 1.1\left(\frac{M - M_{dr}}{1 - M_{dr}}\right)^3. \tag{21}$$

The calculations performed with the use of dependences (16) – (21) in comparison with the experimental data for the symmetrical NACA 0006 – 0018 airfoils at the Mach numbers $M = 0.3 - 0.8$ provide a good coincidence. The design of propeller with regard for air compressibility is significantly simplified by obtaining and verification of such dependences for the blade airfoils being chosen. The Reynolds number has no effect on geometrical characteristics of the optimal propeller at $\mathrm{Re} = 3 \times 10^6$. The decrease of Re number results in the increase of chord only in the zones of low Reynolds numbers.

The critical number M_{dr} and variation of the Mach number over the span are shown dotted in Fig. 5 for several values of the blade radius. It is seen that the propeller efficiency sharply decreases when the blade zone increases and the Mach number exceeds M_{dr}.

The high-altitude Strato 2C aircraft with the specially-designed five-blade and six meter diameter propeller [8], the parameters of which are presented in the table, was taken for performance evaluation.

Table

Operation altitude	I	II	III	IV
Altitude H, m	12000	18500	22000	24000
Density ρ, kg/m^{-3}	0.30	0.11	0.064	0.047
Flight velocity V, m/s^{-1}	62.2	101.3	131.3	153.8
Mach number	0.21	0.34	0.45	0.52
Twist angle θ_{75}, deg	26.0	43.5	48.5	64.0
Propeller advance ratio, λ	1.088	1.772	2.066	2.418
Revolutions per minute n	572	572	636	636
Power output P, kW	179	298	300	300
Efficiency η	0.87	0.87	0.84	0.64
Perfect efficiency η_{id}	0.96	0.96	0.97	0.97
Propeller thrust (N)				
Evaluated thrust (of perfect propeller [8])	2760	2808	2194	1896
Practical thrust [8]	2502	2556	1909	1252
Evaluated thrust (according to the scheme proposed)	2660	2820	1980	1680

The profile polars for two blade cross-sections are also presented in [8] at $r = 0.6$ and $r = 0.8$ based on which we approximate the following parameters spanwise the blade being designed:

$$C_{Y(\mathrm{I})} = 0.45(1-r) + 0.2r; \quad \varepsilon_{(I)} = 0.036(1-r) + 0.02r;$$

$$C_{Y(\mathrm{II})} = 1.1(1-r) + 0.8r; \quad \varepsilon_{(II)} = 0.0172(1-r) + 0.0102r;$$

$$C_{Y(\mathrm{III})} = 1.2(1-r) + 0.95r; \quad \varepsilon_{(III)} = 0.116(1-r) - 0.004r;$$

$$C_{Y(\mathrm{IV})} = 1.02(1-r) + 0.82r; \quad \varepsilon_{(IV)} = 0.04(1-r) + 0.09r.$$

The design assessment performed showed (see table) that the design thrust of the perfect propeller is within the values for the perfect and real propeller [8] (an exception was case II, in which the design thrust was somewhat higher than the value for the perfect propeller [8].). Figure 6 presents the design characteristics for the perfect propeller for case I.

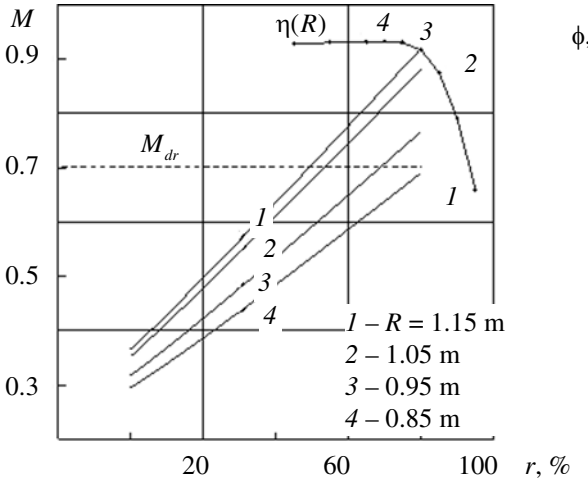

Fig. 5

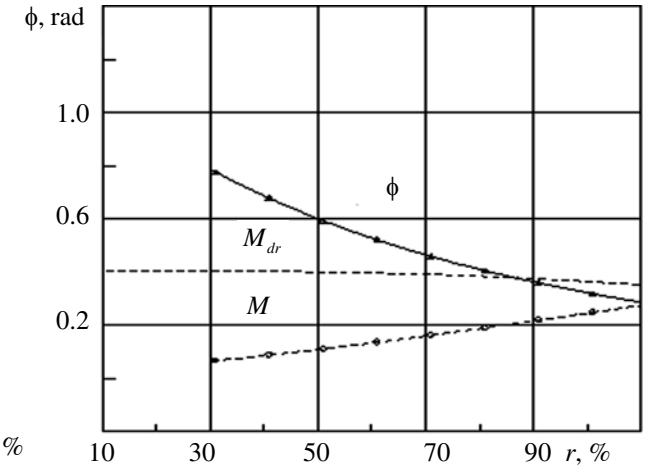

Fig. 6

The technique presented makes it possible to design the perfect propellers for unmanned aerial vehicles with piston engines and may be useful for designers of high-altitude aircraft.

The Visual–Fortran software was used in creating the design assessment program.

REFERENCES

1. Aleksandrov, V.L., *Vozdushnye vinty* (Propellers), Moscow: Oboringiz, 1951.
2. Kravets, A.S., *Kharakteristiki vozduzhnykh vintov* (Propeller Parameters), Moscow: Oborongiz, 1941.
3. Yur'ev, B.N., *Impul'snaya teoriya vozduzhnykh vintov* (Impulse Theory of Propellers), *Trudy VVIA*, no. 306, 1948.
4. Larrabee, E.E., *Practical Design of Minimum Induced Loss Propellers*, SAE International, USA, 1979.
5. Loftin, L.K. Jr. and Smith, H.A., Aerodynamic Characteristics of 15 NACA Airfoil Sections at Seven Reynolds Numbers from 0.7 × 106 to 9.0 × 106, URL: http://naca.central.cranfield.ac.uk/reports/1949/naca–tn–1945.pdf.
6. Martinov, A.K., *Practical Aerodynamics*, Oxford: Pergamon Press, 1965.
7. Wald, Q.R., The Aerodynamics of Propellers, *Progress in Aerospace Sciences*, 2006, vol. 42, no. 2, pp. 85–128.
8. Wichmann, G. and Köster, H., Leistungsnachrechnung des Propellers des Höhenforschungsflugzeugs Strato 2C, DLR-IB 129-96/31, 1996.